ЖЭТФ, 2008, том 133, вып. 3, стр. 544–555

FINAL-STATE RADIATION AND THE POSSIBILITY TO TEST A PION–PHOTON INTERACTION MODEL NEAR THE TWO-PION THRESHOLD

G. Pancheri[a*], *O. Shekhovtsova*[a,b**], *G. Venanzoni*[a***]

[a] *INFN Laboratori Nazionale di Frascati*
00044, Frascati (RM), Italy

[b] *NSC "Kharkov Institute for Physics and Technology", Institute for Theoretical Physics*
61108, Kharkov, Ukraine

Received June 26, 2007

Final-state radiation in the process $e^+e^- \to \pi^+\pi^-$ is considered for the cuts used in the analysis of KLOE data at large angles. By means of the Monte Carlo event generator FEVA, effects of non-point-like behavior of pions are estimated in the framework of the resonance perturbation theory. An additional complication related to the ϕ-meson intermediate state is taken into account and the corresponding contributions (the direct decay $\phi \to \pi^+\pi^-\gamma$ and the double resonance decay $\phi \to \rho^\pm\pi^\mp \to \pi^+\pi^-\gamma$) are added to FEVA. A method to test effects of non-point-like behavior of pions in a model-independent way is proposed.

PACS: 13.25.Jx, 12.39.Fe, 13.40.Gp

1. INTRODUCTION

The ongoing experiments on precise measurements of the cross section of e^+e^- annihilation into hadrons aim at the precision at the 0.5–1.0 % level [1–3]. Such an accuracy is crucial for various tests of the Standard Model [4], e. g., by comparing the experimentally measured value of the muon anomalous magnetic moment a_μ [5] with the theoretical prediction. The accuracy of the theoretical calculation of a_μ is currently limited by the hadronic contribution $a_\mu^{(had)}$. This contribution cannot be reliably calculated in the framework of perturbative QCD because the low-energy region dominates. Fortunately, the leading-order part $a_\mu^{(had;LO)}$ of this contribution can be estimated from the dispersion relation using the experimental cross sections of e^+e^- annihilation as an input [4],

$$a_\mu^{(had;\,LO)} = \Big(\frac{\alpha m_\mu}{3\pi}\Big)^2 \int\limits_{4m_\pi^2}^{\infty} \frac{R(q^2)K(q^2)}{q^4}\,dq^2, \qquad R(q^2) = \frac{\sigma_h(q^2)}{\sigma_\mu(q^2)}, \tag{1}$$

where $\sigma_h(q^2)$ is the total hadronic cross section, $\sigma_\mu(q^2)$ is the total cross section of the process $e^+e^- \to \gamma \to \mu^+\mu^-$, and $K(q^2)$ is a smooth function that increases from 0.63 at the threshold ($s = 4m_\pi^2$) to 1 as $q^2 \to \infty$. The quantity q^2 is the total four-momentum squared of the final hadrons.

This behavior of the integrand results in that the largest contribution (about 70 %) to the leading-order hadronic part of the muon anomalous magnetic moment $a_\mu^{(had;LO)}$ comes from the energy region below or about 1 GeV. Due to the presence of the ρ-meson, the main contribution is related to the $\pi^+\pi^-$ final state.

Experimentally, the energy region from the threshold to the collider beam energy is explored at the Φ-factory DAΦNE (Frascati, $s = 4E^2 = m_\phi^2$) [6, 7] and the B-factories PEP-2 (SLAC, $s = m_{\Upsilon(4S)}^2$) and KEKB (KEK, $s = m_{\Upsilon(4S)}^2$) [8, 9] using the method of radiative return [10–12]. This method relies on the factorization of the radiative cross section into the product

*E-mail: Giulia.Pancheri@lnf.infn.it
**E-mail: shekhovtsova@kipt.kharkov.ua
***E-mail: Graziano.Venanzoni@lnf.infn.it

of the hadronic cross section and a radiation function $H(q^2, \theta_{max}, \theta_{min})$ known from QED [12–14]. The large luminosity of the Φ and B-factories allows compensating the additional factor $\alpha/2\pi$ caused by the hard photon emission. For a two-pion final state considered here, this means that the radiative cross section $\sigma^{\pi\pi\gamma}$ corresponding to the process

$$e^+(p_1) + e^-(p_2) \to \pi^+(p_+) + \pi^-(p_-) + \gamma(k), \qquad (2)$$

can be written as

$$q^2 \frac{d\sigma^{\pi\pi\gamma}}{dq^2} = \sigma^{\pi\pi}(q^2) H(q^2, \theta_{max}, \theta_{min}), \qquad q = p_+ + p_-, \qquad (3)$$

where the hadronic cross section $\sigma^{\pi\pi}$ is taken at a reduced centre-of-mass energy. This factorization is valid only for photon radiation from the initial leptons (initial-state radiation, ISR). This is not possible for final-state (FS) radiation (FSR), which is an irreducible background in radiative return measurements of the hadronic cross section [2, 15][1)]. Indeed, the FSR cross section calculation has an additional complication compared to the ISR case. In principle, radiative corrections caused by ISR, i. e., the function $H(q^2, \theta_{max}, \theta_{min})$, can be calculated in QED, although the accuracy is technically limited. But the situation is different for the FSR cross section because its evaluation relies on models describing the pion–photon interaction. Usually, the combined sQED∗VMD (scalar QED∗Vector meson dominance) model is assumed as a model for calculating the FS bremsstrahlung process [12, 17]. In this case, the pions are treated as pointlike particles (the sQED model) and the total FSR amplitude is multiplied by the pion formfactor estimated in the VMD model. Unfortunately, the sQED∗VMD model is an approximation that is valid for relatively soft photons and can fail for high-energy photons, i. e., near the $\pi^+\pi^-$ threshold. In this energy region, the contributions to FSR beyond the sQED∗VMD model become important. As shown in Ref. [18], the resonance perturbation theory (RPT) is an appropriate model to describe photon–meson interactions in the energy region about 1 GeV, and we use this model to estimate the bremmstrahlung FS contributions beyond sQED.

[1)] In fact, the process of FSR cannot be excluded from the analysis. It can be suppressed by choosing the small-angle kinematics ($\theta_\gamma < \theta_{max} \ll 1$), but increases to 40 % of the ISR for large angles and should then be estimated very carefully. (For some advantages of the large-angle analysis compared to the small-angle one, see [16].)

At the Φ-factory DAΦNE, there is an additional complication related to the possible intermediate ϕ-meson state; the corresponding contributions should be included in the Monte Carlo event generator.

In this paper, we present the results obtained by the Monte Carlo event generator FEVA that simulates process (2) for the DAΦNE accelerator setup. Our computer code FEVA was inspired by MC EVA [12]. The previous version of FEVA was described in [19], where the bremsstrahlung process (in the framework of both RPT and sQED) and the ϕ direct decay (only the f_0 parameterization) were considered. In addition, the current version of FEVA includes the double resonance contribution and a more sophisticated parameterization for the ϕ direct decay.

This paper is organized as follows. In Sec. 2, we give a general description of the FSR process and present the FSR models that are already included in our program FEVA. In Sec. 3, numerical results for the KLOE large-angle analysis are presented. Because most of the effects arising in the FSR are model-dependent, we conclude this paper by suggesting a way to test possible effects beyond sQED, in a model-independent way (see Sec. 4). A conclusion is given in Sec. 5.

2. FINAL-STATE RADIATION MODELS

The cross section of the FSR process can be written as

$$d\sigma_F = \frac{1}{2s(2\pi)^5} \int \delta^4(Q - p_+ - p_- - k) \times \times \frac{d^3p_+ d^3p_- d^3k}{8E_+E_-\omega} |M^{(FSR)}|^2, \qquad (4)$$

where $Q = p_1 + p_2$, $s = Q^2$, and

$$M^{(FSR)} = \frac{e}{s} M^{\mu\nu} \bar{u}(-p_1)\gamma_\mu u(p_2)\epsilon^\star_\nu \qquad (5)$$

and where the FS tensor $M^{\mu\nu}$ describes the transition

$$\gamma^*(Q) \to \pi^+(p_+)\pi^-(p_-)\gamma(k).$$

It is convenient to parameterize the FS tensor in terms of three gauge invariant tensors (see [20] and references [21, 22] therein):

$$M^{\mu\nu}(Q,k,l) \equiv -ie^2 M_F^{\mu\nu}(Q,k,l) = = -ie^2(\tau_1^{\mu\nu} f_1 + \tau_2^{\mu\nu} f_2 + \tau_3^{\mu\nu} f_3), \qquad (6)$$

$$\tau_1^{\mu\nu} = k^\mu Q^\nu - g^{\mu\nu} kQ, \quad l = p_+ - p_-,$$

$$\tau_2^{\mu\nu} = kl(l^\mu Q^\nu - g^{\mu\nu} kl) + l^\nu(k^\mu kl - l^\mu kQ),$$

$$\tau_3^{\mu\nu} = Q^2(g^{\mu\nu}kl - k^\mu l^\nu) + Q^\mu(l^\nu kQ - Q^\nu kl).$$

We emphasize that this expansion is totally model-independent. The model dependence is related only to the explicit form of the scalar functions f_i (we call them structure functions).

Here is the list of the FSR processes included in FEVA MC:

$$e^+ + e^- \to \pi^+ + \pi^- + \gamma, \quad \text{bremsstrahlung process,} \quad (7)$$

$$e^+ + e^- \to \phi \to (f_0; f_0 + \sigma)\gamma \to \pi^+ + \pi^- + \gamma, \quad \phi \text{ direct decay,} \quad (8)$$

$$e^+ + e^- \to \phi \to \rho^\pm \pi^\mp \to \pi^+ + \pi^- + \gamma, \quad \text{VMD contribution,} \quad (9)$$

$$e^+ + e^- \to \rho^\pm \pi^\mp \to \pi^+ + \pi^- + \gamma. \quad (10)$$

In the next sections, we present the models describing these processes. The presence of (8) and (9) is due to the energy at which KLOE is running ($s = m_\phi^2$).

2.1. Bremsstrahlung process

As mentioned in the Introduction, the sQED∗VMD model is an approximation for describing soft photon radiation by pions. To estimate the contributions beyond the sQED∗VMD model, we use the RPT. The model is based on the chiral perturbation theory (χPT) with the explicit inclusion of the vector and axial-vector mesons $\rho_0(770)$ and $a_1(1260)$. Whereas the χPT gives correct predictions for the pion formfactor at very low energy, the RPT is an appropriate framework to describe the pion formfactor at intermediate energies ($E \sim m_\rho$) [18][2)] and satisfies the QCD high-energy behavior.

Using the result in Ref. [20], we write the contribution to the functions f_i (see Eq. (6)) caused by the bremsstrahlung FS process as

$$f_i = f_i^{sQED} + \Delta f_i^{RPT}, \quad (11)$$

$$f_1^{sQED} = \frac{2kQF_\pi(Q^2)}{(kQ)^2 - (kl)^2}, \qquad f_2^{sQED} = \frac{-2F_\pi(Q^2)}{(kQ)^2 - (kl)^2}, \quad (12)$$

$$f_3^{sQED} = 0, \quad (13)$$

where

$$\Delta f_1^{RPT} = \frac{F_V^2 - 2F_V G_V}{f_\pi^2} \times \left(\frac{1}{m_\rho^2} + \frac{1}{m_\rho^2 - s - im_\rho\Gamma_\rho(s)}\right) - \frac{F_A^2}{f_\pi^2 m_a^2} \times \left[2 + \frac{(kl)^2}{D(l)D(-l)} + \frac{(s+kQ)[4m_a^2 - (s + l^2 + 2kQ)]}{8D(l)D(-l)}\right], \quad (14)$$

$$\Delta f_2^{RPT} = -\frac{F_A^2}{f_\pi^2 m_a^2}\,\frac{4m_a^2 - (s + l^2 + 2kQ)}{8D(l)D(-l)}, \quad l = p_+ - p_-, \quad (15)$$

$$\Delta f_3^{RPT} = \frac{F_A^2}{f_\pi^2 m_a^2}\,\frac{kl}{2D(l)D(-l)}, \quad D(l) = m_a^2 - \frac{s + l^2 + 2kQ + 4kl}{4}. \quad (16)$$

For the notation and the details of the calculation, we refer the reader to [20]. F_V, G_V, and F_A are parameters of the model. According to the RPT model, the pion formfactor that includes the ρ–ω mixing can be written as

$$F_\pi(q^2) = 1 + \frac{F_V G_V}{f_\pi^2} B_\rho(q^2)\left(1 - \frac{\Pi_{\rho\omega}}{3q^2} B_\omega(q^2)\right), \quad (17)$$

where

$$B_r(q^2) = \frac{q^2}{m_r^2 - q^2 - im_r\Gamma_r(q^2)}, \quad (18)$$

q^2 is the virtuality of the photon, $f_\pi = 92.4$ MeV, and the parameter $\Pi_{\rho\omega}$ describes the ρ–ω mixing. An energy-dependent width is considered for the ρ meson:

$$\Gamma_\rho(q^2) = \Gamma_\rho \sqrt{\frac{m_\rho^2}{q^2}} \left(\frac{q^2 - 4m_\pi^2}{m_\rho^2 - 4m_\pi^2}\right)^{3/2} \Theta(q^2 - 4m_\pi^2), \quad (19)$$

and a constant width is used for the ω meson, $\Gamma_\omega = 8.68$ MeV and $m_\omega = 782.7$ MeV. We assume that the parameter $\Pi_{\rho\omega}$ that determines the ρ–ω mixing is a constant related to the branching fraction $Br(\omega \to \pi^+\pi^-)$ as

$$Br(\omega \to \pi^+\pi^-) = \frac{|\Pi_{\rho\omega}|^2}{\Gamma_\rho \Gamma_\omega m_\rho^2}. \quad (20)$$

[2)] It was shown in [20] that the coupling constants of the effective chiral Lagrangian at the order p^4 are essentially saturated by the meson resonance exchange.

The values of F_V and G_V as well as the mass of the ρ meson (m_ρ) and the ρ–ω mixing parameter $\Pi_{\rho\omega}$ were estimated by the fit of Novosibirsk CMD-2 data for the pion formfactor [1]:

$$m_\rho = 774.9 \pm 1.4 \text{ MeV}, \quad \Pi_{\rho\omega} = -2774 \pm 291 \text{ MeV}^2,$$

$$\Gamma_\rho = 145.2 \pm 2.6 \text{ MeV}, \quad F_V = 154.2 \pm 0.5 \text{ MeV}.$$

Then $G_V = 64.6 \pm 0.3$ MeV and $Br(\omega \to \pi^+\pi^-) = (0.96 \pm 0.19)\,\%$.

For the a_1 meson, we take $m_a = 1.23$ GeV and $F_A = 0.122$ GeV, which corresponds to the mean value of the experimental decay width $\Gamma(a_1 \to \pi\gamma) = 640 \pm 246$ keV [23].

We note that the contribution of any model describing the bremsstrahlung FS process can be conveniently rewritten as in Eq. (11), and the results should coincide with the sQED∗VMD model prediction in the soft-photon limit.

2.2. ϕ direct decay

For the DAΦNE energy ($s = m_\phi^2$), there are contributions to the final state $\pi^+\pi^-\gamma$ related to the intermediate ϕ meson state. In this section, we consider the direct rare decay $\phi \to \pi^+\pi^-\gamma$.

The ϕ direct decay is assumed to proceed through the intermediate scalar meson state (either f_0 or $f_0{+}\sigma$): $\phi \to (f_0; f_0 + \sigma)\gamma \to \pi^+\pi^-\gamma$, and its mechanism is described by a single formfactor $f_\phi(Q^2)$. As shown in [21, 24], this process affects the formfactor f_1 in Eq. (6):

$$f_1^{scal} = \frac{g_{\phi\gamma} f_\phi(Q^2)}{s - m_\phi^2 + i m_\phi \Gamma_\phi}. \tag{21}$$

First, we consider the case of the f_0 intermediate state. To estimate this contribution, we use the Achasov four-quark model described in [22]: the $\phi \to f_0\gamma$ decay amplitude is generated dynamically through the loop of charged kaons. The formfactor f_ϕ is given by

$$f_\phi^{K^+K^-}(Q^2) = \frac{g_{\phi K^+K^-}}{2\pi^2 m_K^2} \times \\ \times \frac{g_{f_0\pi^+\pi^-} g_{f_0K^+K^-} e^{i\delta_B(Q^2)}}{m_{f_0}^2 - Q^2 + \mathrm{Re}\,\Pi_{f_0}(m_{f_0}^2) - \Pi_{f_0}(Q^2)} \times \\ \times I\left(\frac{m_\phi^2}{m_K^2}, \frac{Q^2}{m_K^2}\right), \tag{22}$$

where $I(.,.)$ is a function known in analytic form [24, 25] and $\delta_B(Q^2) = b\sqrt{Q^2 - 4m_\pi^2}$, with $b = 75^\circ/\text{GeV}$. The term $\mathrm{Re}\,\Pi_{f_0}(m_{f_0}^2) - \Pi_{f_0}(Q^2)$ takes the finite-width corrections to the f_0 propagator into account [22]. A fit to the KLOE data $\phi \to \pi^0\pi^0\gamma$ [3)] gives the following values of the parameters [26]:

$$m_{f_0} = 0.962 \text{ GeV}, \quad \frac{g_{f_0K^+K^-}^2}{4\pi} = 1.29 \text{ GeV}^2, \\ \frac{g_{f_0K^+K^-}^2}{g_{f_0\pi^+\pi^-}^2} = 3.22. \tag{23}$$

In a refined version of this model, which includes the σ meson in the intermediate state [27], the formfactor f_ϕ can be written as

$$f_\phi^{K^+K^-}(Q^2) = \frac{g_{\phi K^+K^-}}{2\pi^2 m_K^2} e^{i(\delta_{\pi\pi}(Q^2) + \delta_{KK}(Q^2))} \times \\ \times I\left(\frac{m_\phi^2}{m_K^2}, \frac{Q^2}{m_K^2}\right) \sum_{R,R'} g_{RK^+K^-} G_{RR'}^{-1} g_{R'\pi^+\pi^-},$$

where $G_{RR'}$ is the matrix of inverse propagators [27]. Such an extension of the model improves the description of the data at low Q^2 (see Fig. 1*a*) and gives the following values of the model parameters [28]:

$$m_{f_0} = 0.977 \text{ GeV}, \quad \frac{g_{f_0K^+K^-}^2}{4\pi} = 1.12 \text{ GeV}^2, \\ \frac{g_{f_0K^+K^-}^2}{g_{f_0\pi^+\pi^-}^2} = 6.9, \tag{24}$$

$$m_\sigma = 0.462 \text{ GeV}, \quad \frac{g_{\sigma K^+K^-}^2}{4\pi} = 0.024 \text{ GeV}^2, \\ \frac{g_{\sigma K^+K^-}^2}{g_{\sigma\pi^+\pi^-}^2} = 0.052. \tag{25}$$

2.3. VMD contribution

Another contribution producing the intermediate ϕ meson state is the double resonance contribution in (9). In this case, the off-shell ϕ meson decays to $\rho^\pm$ and $\pi^\mp$, which is followed by $\rho \to \pi\gamma$. The explicit value of the functions f_i^{VMD} for this decay can be found in Ref. [21]. To maintain correspondence with the KLOE analysis in [28], we also added the additional phase between

[3)] $\Gamma(f_0 \to \pi^+\pi^-) = \frac{2}{3}\Gamma(f_0 \to \pi\pi)$.

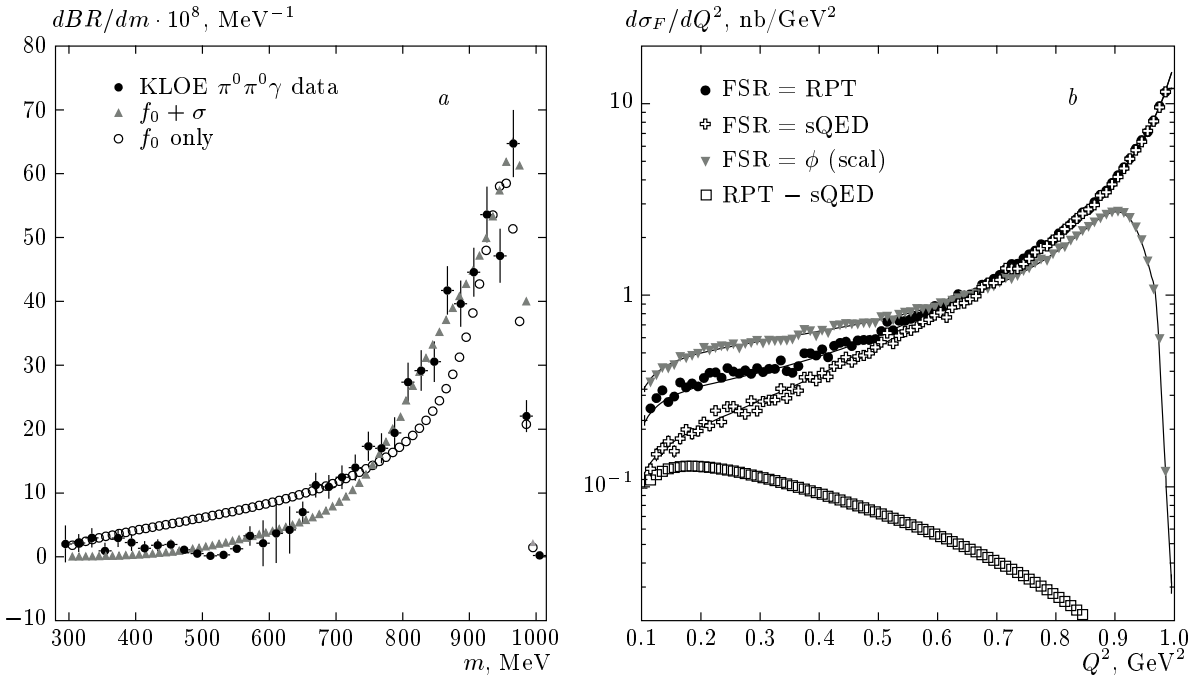

Fig. 1. *a*) The dependence of the branching ratio of the ϕ direct decay on the intermediate scalar states. *b*) Contribution to the FSR cross section $d\sigma_F/dQ^2$ in the region $0 \le \theta_\gamma \le 180^\circ$, $0 \le \theta_\pi \le 180^\circ$ at $s = m_\phi^2$. RPT is represented by circles, sQED by crosses, ϕ by triangles, and the difference between RPT and sQED is indicated by squares

VMD and ϕ direct contributions, the factor Π_ρ^{VMD} [4)] and the phase of the ω–ϕ meson mixing $\beta_{\omega\phi}$:

$$
\begin{aligned}
f_1^{VMD} &= -\frac{1}{4\pi\alpha s}\Big((-1+\frac{3}{2}x+\sigma)(g(x_1)+g(x_2))+ \\
&\quad + \frac{1}{4}(x_1-x_2)(g(x_1)-g(x_2))\Big), \\
f_2^{VMD} &= -\frac{1}{4\pi\alpha s^2}(g(x_1)+g(x_2)), \\
f_3^{VMD} &= -\frac{1}{8\pi\alpha s^2}(g(x_1)-g(x_2)),
\end{aligned}
\tag{26}
$$

where

$$
g(x) = \frac{e g_{\rho\pi}^{\phi} g_{\pi\gamma}^{\rho}}{4F_\phi}\,\frac{m_\phi^2 e^{i\beta_\rho} e^{i\beta_{\omega\phi}}}{s - m_\phi^2 + i m_\phi \Gamma_\phi} \times \\
\times \frac{s^2 \Pi_\rho^{VMD}}{(1-x)s - m_\rho^2 + i m\rho \Gamma_\rho((1-x)s)} \tag{27}
$$

with

$$
x_{1,2} = \frac{2p_{+,-}(p_1+p_2)}{s}, \quad x = 2 - x_1 - x_2.
$$

The quantities $g_{\rho\pi}^{\phi}$ and $g_{\pi\gamma}^{\rho}$ are the respective coupling constants determining the $\phi \to \rho\pi$ and $\rho \to \pi\gamma$ vertices,

$$
F_\phi = \sqrt{\frac{3\Gamma(\phi \to e^+e^-)}{\alpha m_\phi}},
$$

and $e = \sqrt{4\pi\alpha}$. A fit to the KLOE data for $\phi \to \pi^0\pi^0\gamma$ [28] gives

$$
\begin{gathered}
g_{\rho\pi}^{\phi} = 0.811 \text{ GeV}^{-1}, \quad g_{\pi\gamma}^{\rho} = 0.295 \text{ GeV}^{-1}, \\
F_\phi = 42.5, \quad \Pi_\rho^{VMD} = 0.58195, \\
\beta_\rho = 32.996^\circ, \quad \beta_{\omega\phi} = 163^\circ.
\end{gathered}
\tag{28}
$$

2.4. Other contributions

We included in our program the channel $\gamma^* \to \to \rho^\pm\pi^\mp \to \pi^+\pi^-\gamma$ [5)], whose amplitude has been evaluated in RPT model. To write this part of FSR, we used the results in Ref. [20] for the function $f_i^{\rho^\pm}$:

[4)] Including Π_ρ^{VMD}, we rescale the coupling constant. In our opinion, this rescales the constant $g_{\rho\pi}^{\phi}$ that cannot be directly determined from any experimental decay width.

[5)] In the energy region $s \le m_\phi^2$, this direct transition $\gamma^* \to \rho^\pm\pi^\mp$ can be regarded as the tail of the double resonance contribution of the ρ' meson decay: $\gamma^* \to \rho' \to \rho\pi$ for $s = m_\phi^2$.

$$\Delta f_1^{\rho^\pm} = \frac{8H_V^2}{9f_\pi^2}\left[(kQ+l^2)\left(\frac{1}{C(l)}+\frac{1}{C(-l)}\right)+ \right.$$
$$\left. +2kl\left(\frac{1}{C(l)}-\frac{1}{C(-l)}\right)\right]+\frac{64H_V^2}{9f_\pi^2}, \quad (29)$$

$$\Delta f_2^{\rho^\pm} = -\frac{8H_V^2}{9f_\pi^2}\left(\frac{1}{C(l)}+\frac{1}{C(-l)}\right), \quad (30)$$

$$\Delta f_3^{\rho^\pm} = \frac{8H_V^2}{9f_\pi^2}\left(\frac{1}{C(l)}-\frac{1}{C(-l)}\right), \quad (31)$$

where

$$C(\pm l) = m_\rho^2 - (k+p_\pm)^2 - im_\rho\Gamma_\rho((k+p_\pm)^2)$$

with

$$(k+p_\pm)^2 = \frac{Q^2+l^2+2kQ\pm 4kl}{4}.$$

The value of the constant H_V is determined by the width of the $\rho\to\pi\gamma$ decay

$$\Gamma(\rho^\pm\to\pi^\pm\gamma) = \frac{4\alpha m_\rho^3 H_V^2}{27f_\pi^2}\left(1-\frac{m_\pi^2}{m_\rho^2}\right)^3$$

and can be related to the constant $g_{\pi\gamma}^\rho$ as

$$H_V = \frac{3f_\pi g_{\pi\gamma}^\rho}{4\sqrt{2}}.$$

This gives $H_V = 0.0144$. In agreement with the calculation in [20], we found a negligible contribution of this channel; for simplicity, we discard its effects on the numerical results presented in the next section.

3. NUMERICAL RESULTS

In this section, we present the results for the differential cross section and the forward–backward asymmetry [12, 29] for the reaction $e^+e^-\to\pi^+\pi^-\gamma$, where the FSR amplitude (M_{FSR}) receives contributions from both RPT (M_{RPT}) and the $\phi\to\pi^+\pi^-\gamma$ decay (M_ϕ). The last one is a sum of the ϕ direct decay (M_ϕ^{scal}) and VMD (M_ϕ^{VMD}) contributions. Thus, the total contribution $d\sigma_T$ of process (2) can be written as

$$d\sigma_T = d\sigma_I + d\sigma_F + d\sigma_{IF} \sim |M_{ISR}+M_{FSR}|^2, \quad (32)$$

$$d\sigma_I \sim |M_{ISR}|^2,$$
$$d\sigma_F \sim |M_{RPT}|^2 + |M_\phi|^2 + 2\,\mathrm{Re}\{M_{RPT}M_\phi^*\},$$
$$d\sigma_{IF} \sim 2\,\mathrm{Re}\{M_{ISR}(M_{RPT}+M_\phi)^*\},$$

where $d\sigma_I$ corresponds to the ISR cross section and $d\sigma_F$ to the FSR one. The interference term $d\sigma_{IF}$ is equal to zero for symmetric cuts on the polar angle of the pions [7].

The different contributions to the FSR differential cross section $d\sigma_F$, evaluated at $s = m_\phi^2$, are shown in Fig. 1*b* for the full angular range $0\le\theta_\gamma\le 180^\circ$, $0\le\theta_\pi\le 180^\circ$. Good agreement between the results of the Monte Carlo simulation (points) and the analytic prediction (solid line) is found. It can be noted that at low Q^2, the contribution from the direct ϕ decay (i. e., the term proportional to $|M_\phi^{scal}|^2$ in Eq. (32)) is quite large, and therefore the additional contribution beyond sQED can be revealed only in the case of destructive interference between the two amplitudes ($\mathrm{Re}(M_{RPT}M_\phi^*)<0$). Published data from the KLOE experiment [30] are in favor of this assumption, which we use in what follows.

We first consider the case $s = m_\phi^2$. In Fig. 2, we show the values of the differential cross section $d\sigma_T/d\sigma_I$ and the forward–backward asymmetry for the angular cuts of the KLOE large-angle analysis [16, 30]:

$$50^\circ\le\theta_\gamma\le 130^\circ,$$
$$50^\circ\le\theta_\pi\le 130^\circ \quad (33)$$

for the bremsstrahlung FS process in the framework of the sQED∗VMD model and with the ϕ decay contributions (VMD and the ϕ direct decay), for a hard photon radiation with energies $E_\gamma > 20$ MeV.

Figure 3 shows the effects of RPT and ϕ direct decay terms on the total differential cross section and their contribution to the FSR cross section for angular cuts (33). Several distinctive features can be noted: 1) the peak at about 1 GeV^2 corresponds to the f_0 intermediate state for the direct $\phi\to\pi\pi\gamma$ amplitude; 2) the presence of RPT terms in the FSR is relevant at low Q^2, where they make an additional contribution up to 40 % to the ratio $d\sigma_{RPT+\phi}/d\sigma_{sQED+\phi}$ (as shown in Fig. 3*a,b*); 3) the destructive interference between the ϕ decay and the bremsstrahlung FS process reduces the visible cross section in the whole Q^2 range and its dependence on FS bremsstrahlung model at low Q^2 (see Fig. 2*b*). We also draw attention to the VMD contribution. As we can see from Fig. 2, the VMD contribution leaves the value of the differential cross section almost unchanged (Fig. 2*a,b*), but it essentially changes the value of the forward–backward asymmetry (Fig. 2*c*) and follows the experimental data for it. Last but not least, all contributions beyond sQED are large enough near the threshold to make the analysis difficult.

To reduce the background from the ϕ decay in the measurement of the pion formfactor at the threshold, KLOE has taken more than 200 pb^{-1} of data

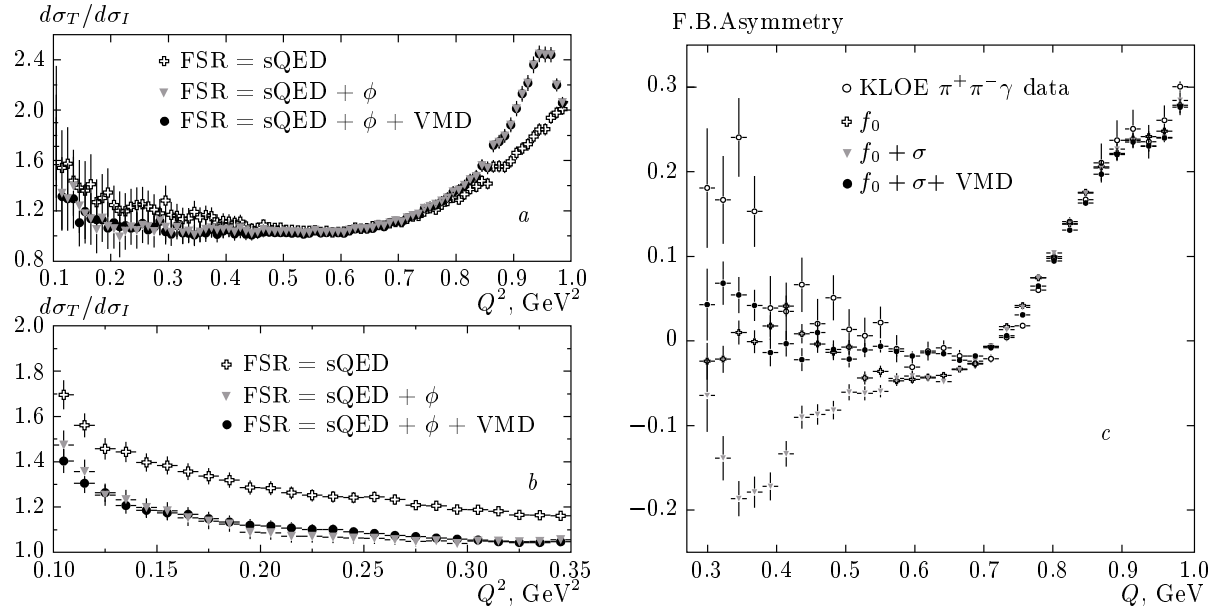

Fig. 2. The ratio $d\sigma_T/d\sigma_I$ of the total cross section to the ISR one (a,b) and the forward–backward asymmetry (b,c) as a function of the invariant mass of the two pions, when the ϕ contribution is taken into account and the bremsstrahlung process is in the framework of the sQED∗VMD model. The angular region is $50^\circ \le \theta_\gamma \le 130^\circ$, $50^\circ \le \theta_\pi \le 130^\circ$ and $s = m_\phi^2$

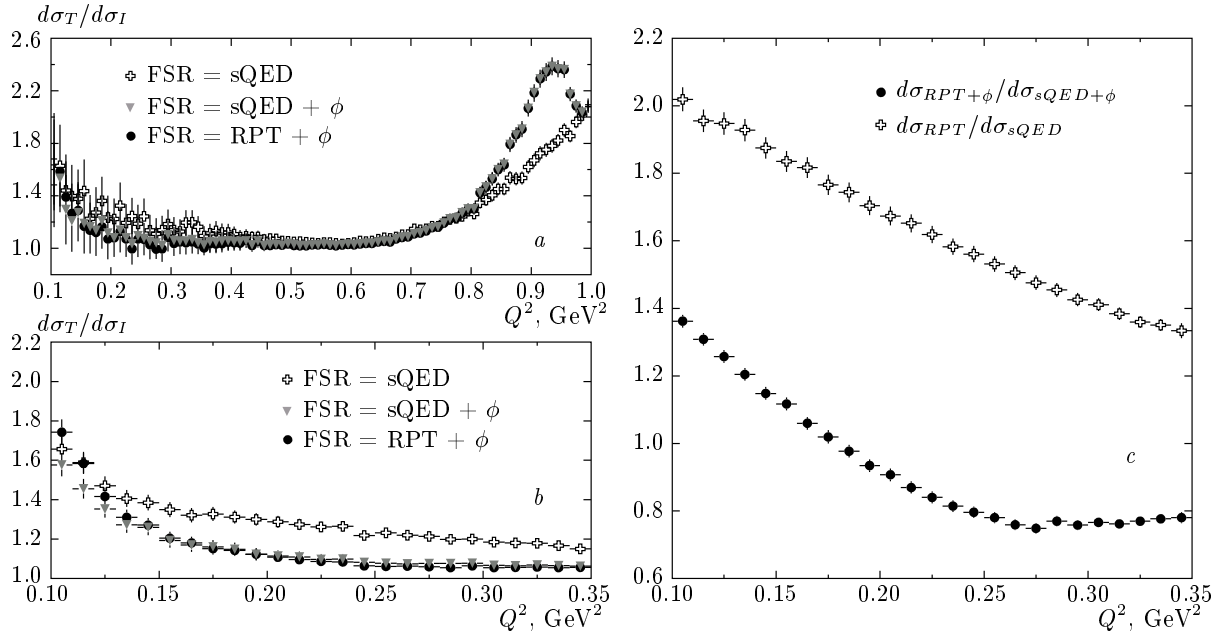

Fig. 3. The ratio $d\sigma_T/d\sigma_I$ (a,b) as a function of the invariant mass of the two pions for different models describing the bremsstrahlung FS process (either RPT or sQED∗VMD) and the ratio of the FSR cross section in the framework of RPT to the sQED cross section, when the ϕ direct decay contribution is (or is not) taken into account (c), in the region $50^\circ \le \theta_\gamma \le 130^\circ$, $50^\circ \le \theta_\pi \le 130^\circ$ at $s = m_\phi^2$

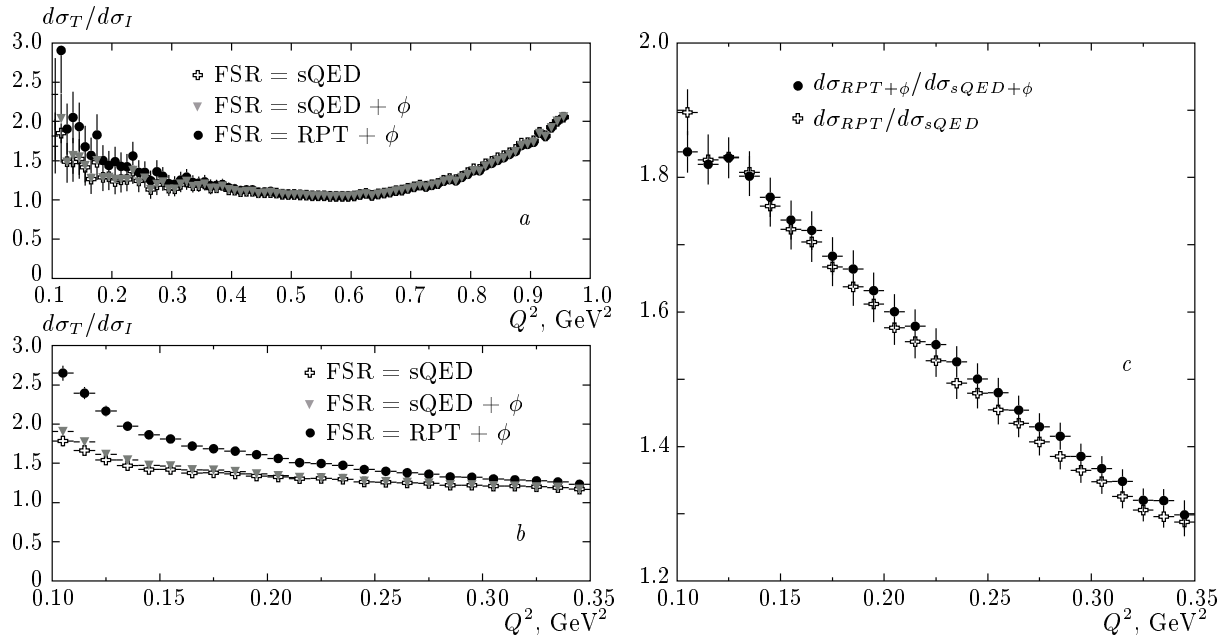

Fig. 4. The same ratio as in Fig. 3 at $s = 1$ GeV^2

at 1 GeV [31]. In this case, the ϕ-meson intermediate contributions are suppressed (in Fig. 4*c*, the values of $d\sigma_T$ with and without the ϕ decay almost coincide) and the main contribution to FSR comes from the bremsstrahlung process (see Sec. 2.1), allowing a model for it to be studied.

4. MODEL-INDEPENDENT TEST OF FSR MODELS

Contributions to the bremsstrahlung FS process beyond sQED, as in the case of RPT, can lead to sizeable effects on the cross section and asymmetry at the threshold, as shown in Figs. 2–4. Precise measurement of the pion formfactor in this region is needed to control them at the required level of accuracy. This looks like a rather difficult task, considering that effects beyond sQED, as well as the contribution from $\phi \to \pi^+\pi^-\gamma$, are model-dependent.

One can think of constructing a general amplitude for $e^+e^- \to \pi^+\pi^-\gamma$ in accordance with some underlying theory and then try to determine the free parameters by a constrained fit on specific variables (like the mass spectrum, charge and forward–backward asymmetry, angular distribution, etc.). In particular, the charge asymmetry has been proved to be a powerful tool to discriminate between different models of $\phi \to \pi^+\pi^-\gamma$ [29]. However, when the number of the parameters is large, correlations between the parameters of the model can arise and spoil the effective power of these fits. The situation becomes even worse if the pion formfactor also has to be extracted from the same data. As an example, if we consider only the ρ and ω contribution to the pion formfactor and the ρ and a_1 contribution to FSR in the case of the RPT model, the number of free parameters is already six. The presence of the ϕ direct and VMD decays results in additional free parameters.

The possibility to determine some of the parameters by external data can strongly help, as in the case of the $\phi \to \pi^+\pi^-\gamma$ amplitude, which can be determined by the $\pi^0\pi^0\gamma$ channel copiously produced at DAΦNE. An additional source of information to be used for determining the contributions to FSR beyond sQED in a model-dependent way is the dependence of the FSR amplitude on the e^+e^- invariant mass squared s.

We write the differential cross section for the emission of one photon in the process $e^+e^- \to \pi^+\pi^-\gamma$ as a function of the invariant mass of the two pions:

$$\left(\frac{d\sigma_T}{dQ^2}\right)_s = |F_\pi(Q^2)|^2 H_s(Q^2) + \left(\frac{d\sigma_F}{dQ^2}\right)_s, \qquad (34)$$

where $\left(\dfrac{d\sigma_F}{dQ^2}\right)_s$ is the differential cross section for the emission of a photon in the final state and the ISR function $H_s(Q^2)$ was defined in the Introduction. We use a subscript s to indicate the dependence of each quantity

on the e^+e^- invariant mass s. Because we consider only symmetric angular cuts for pions, the interference term between initial- and final-state radiation is neglected.

At relatively high Q^2, the FSR differential cross section $\left(\frac{d\sigma_F}{dQ^2}\right)_s$ is dominated by the contribution coming from sQED (M_{sQED}) and ϕ direct decay (M_ϕ):

$$\left(\frac{d\sigma_{sQED+\phi}}{dQ^2}\right)_s \sim |M_{sQED}+M_\phi|^2. \tag{35}$$

Contributions beyond sQED (ΔM) are expected to be important at low Q^2. They introduce an additional term (ΔM) in the above expression:

$$\left(\frac{d\sigma_F}{dQ^2}\right)_s \sim |M_{sQED}+\Delta M+M_\phi|^2 = \tag{36}$$

$$= |M_{sQED}+M_\phi|^2 + |\Delta M|^2 + $$

$$+ 2\,\mathrm{Re}\left\{\Delta M (M_{sQED}+M_\phi)^*\right\}. \tag{37}$$

We now consider the quantity

$$Y_s(Q^2) = \frac{\left(\frac{d\sigma_T}{dQ^2}\right)_s - \left(\frac{d\sigma_{sQED+\phi}}{dQ^2}\right)_s}{H_s(Q^2)} = $$

$$= |F_\pi(Q^2)|^2 + \Delta F_s(Q^2), \tag{38}$$

where

$$\Delta F_s \sim \left(|\Delta M|^2 + 2\,\mathrm{Re}\left\{\Delta M (M_{sQED}+M_\phi)^*\right\}\right)_s \frac{1}{H_s}.$$

If no contribution beyond sQED is present ($\Delta M = 0$), $Y_s(Q^2)$ coincides with the square of the pion formfactor, independently of the energy $\sqrt{s}$ at which it is evaluated, while any dependence on s is only due to an additional contribution to FSR beyond sQED. In particular, the difference of $Y_s(Q^2)$ computed at two beam energies s_1 and s_2 can only come from FSR beyond sQED:

$$\Delta Y(Q^2) = Y_{s_1}(Q^2) - Y_{s_2}(Q^2) = $$

$$= \Delta F_{s_1}(Q^2) - \Delta F_{s_2}(Q^2). \tag{39}$$

Therefore, before extracting the pion formfactor at the threshold, we suggest to look at the difference $\Delta Y(Q^2)$, which can be used to estimate the contribution beyond sQED to the FSR amplitude in a model-independent way.

As a realistic application of this procedure, we consider the case of DAΦNE, where KLOE has already collected more than 200 pb^{-1} at 1 GeV^2 and 2.5 fb^{-1} at m_ϕ^2, which, in the range $Q^2 < 0.35$ GeV^2, respectively correspond to $O(10^3)$ and $O(10^4)$ events, in the region $50^\circ \le \theta_\gamma \le 130^\circ$, $50^\circ \le \theta_\pi \le 130^\circ$. We consider RPT as a model for the effects beyond sQED.

Figure 5*a*, shows the quantity $Y_s(Q^2)$ at $s_1 = 1$ GeV^2 and at $s_2 = m_\phi^2$ when no additional RPT term is included in FSR. As expected, each of these quantities coincides with the square of the pion formfactor $|F_\pi(Q^2)|^2$, shown by a solid line. The difference $\Delta Y(Q^2)$ is shown in Fig. 5*b*, which is consistent with zero as expected. In the region $s < 0.35$ GeV^2, we can expand the pion formfactor as in [4]:

$$F_\pi(q^2) \approx 1 + p_1 q^2 + p_2 q^4. \tag{40}$$

Using the same experimental data for the pion formfactor [1] as before, we have $p_1 = 1.15 \pm 0.06$ GeV^{-2}, $p_2 = 9.06 \pm 0.25$ GeV^{-4}, and $\chi^2/\nu \approx 0.13$. A combined fit of $Y_s(Q^2)$ to the pion formfactor gives the values $p_1 = 1.4 \pm 0.2$ GeV^{-2}, $p_2 = 8.8 \pm 0.7$ GeV^{-4}, and $\chi^2/\nu = 0.25$, which are in a reasonable agreement with the results in (40).

The situation is different as soon as the bremsstrahlung FS process is modeled by RPT. In this case, as shown in Fig. 6*b*, the difference $\Delta Y(Q^2) \neq 0$ and the quantities $Y_s(Q^2)$ can no longer be identified with $|F_\pi(Q^2)|^2$ (see Fig. 6*a*) [6].

Before concluding, we list the main points of our method.

1. The quantity $\left(\frac{d\sigma_{sQED+\phi}}{dQ^2}\right)_s$ is an input parameter of our procedure and can be computed numerically by Monte Carlo simulations.

2. The amplitude for $\phi \to \pi^+\pi^-\gamma$ is taken from the $\pi^0\pi^0\gamma$ channel.

3. The missing ISR multi-photon radiative correction can be added to H_s and does not spoil the effective power of the method.

4. A clear advantage of the procedure based on a Monte Carlo event generator is that it allows keeping control over the efficiency and resolution of the detector and fine tuning of the parameters.

Even if the main limitation of the method could come from the uncertainty on the parameters of the $\phi \to \pi^+\pi^-\gamma$ amplitude, especially at low Q^2, we believe that the KLOE data on $\phi \to \pi^0\pi^0\gamma$ will allow a precise description of this amplitude. In any case, in agreement with [29], we strongly recommend to check the amplitude by using charge asymmetry and to compare it with the spectrum of $\pi^+\pi^-\gamma$, at least at high

[6] Destructive interference between the RPT and $\phi \to \pi^+\pi^-\gamma$ amplitudes tends to cancel the effects beyond sQED at $s = m_\phi^2$ (see Fig. 3*a*,*b*). Therefore, the quantity $Y_s(Q^2)$ almost coincides with the pion formfactor.

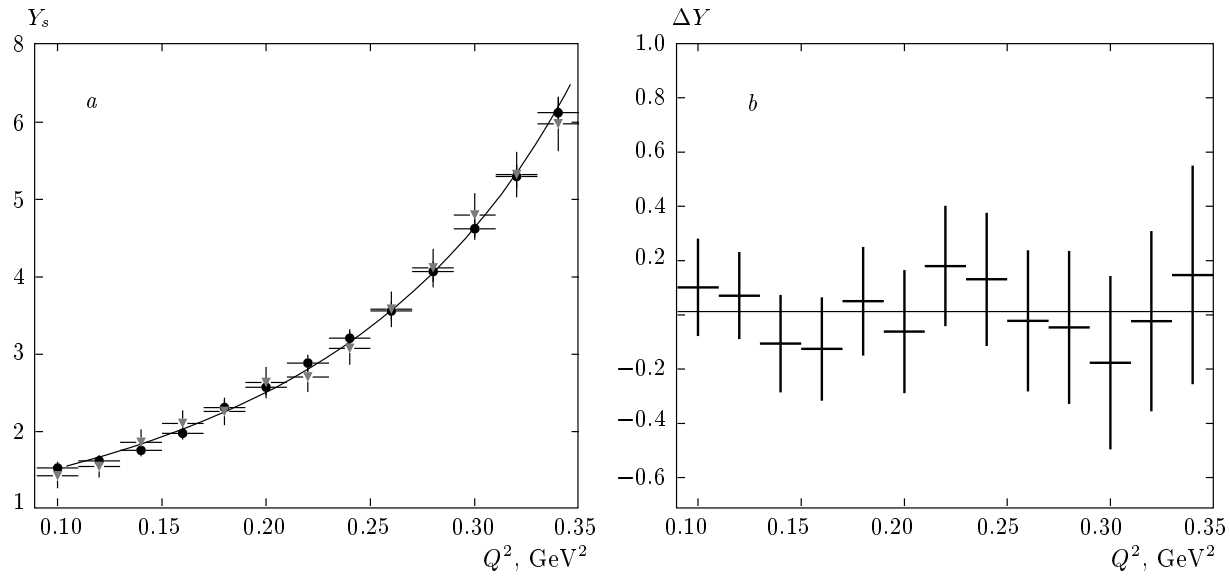

Fig. 5. *a*) $Y_s(Q^2)$ at $s = 1$ GeV^2 (triangles) and at $s = m_\phi^2$ (circles), when FSR includes only the sQED and ϕ contribution. The pion formfactor $|F_\pi(Q^2)|^2$ is shown by a solid line. *b*) The difference $\Delta Y(Q^2)$

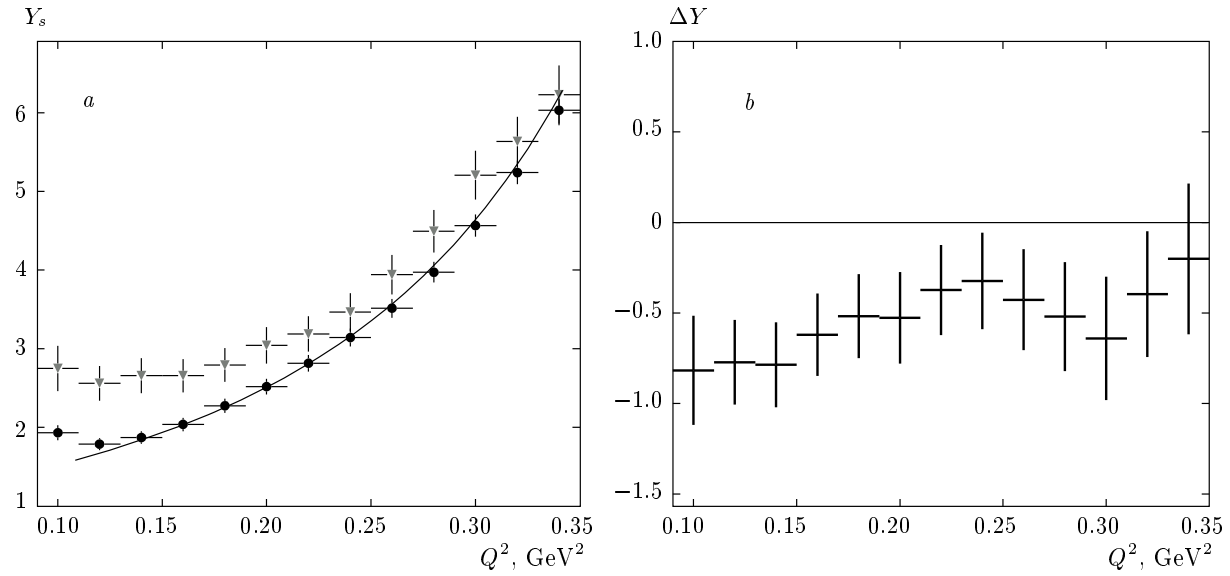

Fig. 6. *a*) $Y_s(Q^2)$ at $s = 1$ GeV^2 (triangles) and at $s = m_\phi^2$ (circles), when FSR includes the RPT and ϕ contributions. The pion formfactor $|F_\pi(Q^2)|^2$ is shown by a solid line. *b*) The difference $\Delta Y(Q^2)$

Q^2, where the point-like approximation is safe (as done in [30]).

5. CONCLUSION

A test of FSR at the threshold in the process $e^+e^- \to \pi^+\pi^-\gamma$ is a rather important issue, not only for the role of FSR as a background to the measurement of the pion formfactor but also to obtain information about pion–photon interactions when the intermediate hadrons are far off the mass shell. At $s = m_\phi^2$, an additional complication arises: the presence of the decay $\phi \to \pi^+\pi^-\gamma$, which occurs either through the intermediate scalar (the direct ϕ decay) or the vector state (VMD contribution), whose amplitude and relative phase can be described according to some

model. By means of the Monte Carlo event generator FEVA, which also includes the contribution of the rare $\phi \to \pi^+\pi^-\gamma$ decay, we estimate the effects beyond sQED in the framework of RPT for angular cuts used in the KLOE analysis of the pion formfactor at the threshold. We show that the low-Q^2 region is sensitive both to the inclusion of additional terms in the FSR amplitude given by the RPT model and to the ϕ decay contribution (especially its VMD part).

We also propose a method that allows estimating the effects beyond sQED in a model-independent way. We found that the deviation from sQED predicted by RPT can be observed within the current KLOE statistics.

We emphasize once again that this work was motivated by the ongoing experiment on precise measurements of the muon anomalous magnetic moment [32], which allows testing the Standard Model with a fabulous precision.

It is a pleasure to thank all our colleagues of the "Working Group on Radiative Corrections and MC Generators for Low Energies" for many useful discussions [33]. We are especially grateful to S. Eidelman for the useful discussion and careful reading of the manuscript. This work was supported by the INTAS (grant № 05-1000008-8328). G. P. also acknowledges support from EU-CT2002-311 Euridice contract.

REFERENCES

1. R. R. Akhmetshin, V. M. Aulchenko, V. Banzarov et al. [CMD-2 Collaboration], Phys. Lett. B **648**, 28 (2007).

2. A. Aloisio, F. Ambrosino, A. Antonelli et al. [KLOE Collaboration], Phys. Lett. B **606**, 12 (2005).

3. M. N. Achasov, K. I. Beloborodov, A. V. Berdyugin et al. [SND Collaboration], Zh. Eksp. Teor. Fiz. **130**, 437 (2006).

4. S. Eidelman and F. Jegerlehner, Z. Phys. C **67**, 585 (1995).

5. G. W. Bennett, B. Bousquet, H. N. Brown et al., Phys. Rev. D **73**, 072003 (2006).

6. G. Cataldi, A. G. Denig, W. Kluge, S. Müller, and G. Venanzoni, in *Proc. Physics and Detectors for DAΦNE*, Frascati, Italy (1999), p. 569; A. Aloisio, F. Ambrosino, A. Antonelli et al. [KLOE Collaboration], E-print archives, hep-ex/0107023.

7. S. Spagnolo, Europ. Phys. J. C **6**, 637 (1999); A. Aloisio, F. Ambrosino, A. Antonelli et al. [KLOE Collaboration], E-print archives, hep-ex/0312056.

8. E. P. Solodov [BABAR Collaboration], E-print archives, hep-ex/0107027; G. Sciolla [BABAR Collaboration], Nucl. Phys. B–Proc. Suppl. **99**, 135 (2001); N. Berger, E-print archives, hep-ex/0209062.

9. M. Benayoun, S. I. Eidelman, V. N. Ivanchenko, and Z. K. Silagadze, Mod. Phys. Lett. A **14**, 2605 (1999).

10. Min-Shin Chen and P. M. Zerwas, Phys. Rev. D **11**, 58 (1975).

11. A. B. Arbuzov, E. A. Kuraev, N. P. Merenkov, and L. Trentadue, JHEP **12**, 009 (1998); M. Konchatnij and N. P. Merenkov, Pis'ma Zh. Eksp. Teor. Fiz. **69**, 769 (1999).

12. S. Binner, J. H. Kühn, and K. Melnikov, Phys. Lett. B **459**, 279 (1999); J. Kühn, Nucl. Phys. B–Proc. Suppl. **98**, 2 (2001).

13. V. N. Baier and V. A. Khoze, Zh. Eksp. Teor. Fiz. **48**, 946, 1708 (1965).

14. V. A. Khoze, M. I. Konchatnij, N. P. Merenkov et al., Europ. Phys. J. C **25**, 199 (2002).

15. H. Czyż, A. Grzelińska, J. H. Kühn, and G. Rodrigo, Europ. Phys. J. C **33**, 333 (2004).

16. D. Leone, Nucl. Phys. B–Proc. Suppl. **162**, 95 (2006).

17. H. Czyż, A. Grzelinska, J. H. Kühn, and G. Rodrigo, Europ. Phys. J. C **27**, 563 (2003).

18. G. Ecker, J. Gasser, A. Pich, and E. de Rafael, Nucl. Phys. B **321**, 311 (1989); G. Ecker, J. Gasser, H. Leutwyler, A. Pich, and E. de Rafael, Phys. Lett. B **223**, 425 (1989).

19. G. Pancheri, O. Shekhovtsova, and G. Venanzoni, Phys. Lett. B **642**, 342 (2006).

20. S. Dubinsky, A. Korchin, N. Merenkov, G. Pancheri, and O. Shekhovtsova, Europ. Phys. J. C **40**, 41 (2005).

21. G. Isidori, L. Maiani, M. Nicolaci, and S. Pacetti, JHEP 0605:049 (2006).

22. N. N. Achasov, V. V. Gubin, and E. P. Solodov, Phys. Rev. D **55**, 2672 (1997).

23. S. Eidelman, K. G. Hayes, K. A. Olive et al. [Particle Data Group], Phys. Lett. B **592**, 1 (2004).

24. K. Melnikov, F. Nguyen, B. Valeriani, and G. Venanzoni, Phys. Lett. B **477**, 114 (2000).

25. F. E. Close, N. Isgur, and S. Kumano, Nucl. Phys. B **389**, 513 (1993); J. L. Lucio Martinez and M. Napsuciale, Phys. Lett. B **331**, 418 (1994).

26. A. Aloisio, F. Ambrosino, A. Antonelli et al. [KLOE Collaboration], Phys. Lett. B **537**, 21 (2002).

27. N. N. Achasov and A. V. Kiselev, Phys. Rev. D **73**, 054029 (2006).

28. F. Ambrosino, A. Antonelli, M. Antonelli et al. [KLOE Collaboration], Europ. Phys. J. C **49**, 473 (2007).

29. H. Czyż, A. Grzelinska, and J. H. Kühn, Phys. Lett. B **611**, 116 (2005).

30. F. Ambrosino, A. Antonelli, M. Antonelli et al. [KLOE Collaboration], Phys. Lett. B **634**, 148 (2006).

31. A. Denig, Nucl. Phys. B–Proc. Suppl. **162**, 81 (2006); S. Müller, *PhD Thesis*, www-ekp.physik.uni-karlsruhe.de/pub/web.

32. R. M. Carey et al., *Proposal of the BNL Experiment E969* (2004), www.bnl.gov/henp/docs/pac0904/P969.pdf; B. I. Roberts, E-print archives, hep-ex/0501012.

33. "*Working Group on Radiative Corrections and MC Generators for Low Energies*", http://www.lnf.infn.it/wg/sighad.